The International Journal of Artificial Organs / Vol. 24 / no. 5, 2001 / pp. 304-310

Biomaterials

Design and analysis of coupling methods for modular endoprosthetic systems as an alternative to the conical coupling

R.P.J. POLMANS[1], H.J. GROOTENBOER[2], H. SCHRAFFORDT KOOPS[3], R.P.H. VETH[4], J.R. van HORN[5], G.J. VERKERKE[1]

[1] University of Groningen, Department of Biomedical Engineering, Groningen - The Netherlands
[2] University of Twente, Department of Biomechanics, Enschede - The Netherlands
[3] University Hospital Groningen, Department of Surgical Oncology, Groningen - The Netherlands
[4] University Hospital Nijmegen, Department of Orthopedics, Nijmegen - The Netherlands
[5] University Hospital Groningen, Department of Orthopedics, Groningen - The Netherlands

ABSTRACT: Modular endoprostheses are often used in bone tumor management. However, the conical coupling that connects the various modules has several shortcomings. As an alternative, four new couplings have been developed. To find out if they have sufficient strength and show no movement during loading, each coupling was analysed using the finite element method. Bolt force and friction coefficient was varied to examine their influence.
From the analysis it was concluded that coupling B, a dovetail coupling, meets all requirements and is the best alternative to the conical coupling. Sensitivity to bolt force and friction coefficient is very limited. (Int J Artif Organs 2001; 24: 304-10)

KEY WORDS: Endoprosthesis, FEM, Modular, Coupling, Tumor

INTRODUCTION

Patients with a bone tumor can be treated by resecting the affected bone and implanting a metal endoprosthesis to bridge the defect (1, 2). Depending on the size and location of the tumor the proximal tibia and/or the distal femur and/or the total femur must be replaced.

When children have to undergo bone replacement the other, normal leg grows more than the resected leg, which could result in an unacceptable leg length difference. Therefore, endoprostheses have been developed that contain a lengthening element to match the growth of the other leg (3-8). Modularity of the femoral component started with the desire to be able to control prosthetic length during tumor surgery. The main advantage of a modular prostheses is that it can cope with individual circumstances during surgery (9-12). A modular prosthetic system provides the surgeon with the possibility of determining the adequate amount of resection intraoperatively. A growing endoprosthesis modularity makes it possible to replace the lengthening element by a solid part when the patient stops growing without replacing the entire prosthesis.

Currently, only one type of modular coupling is applied in all modular endoprosthetic systems, the conical coupling (11, 13, 14). The coupling system of the Endo-Modell® modular endoprosthetic system (Waldemar Link, Lübeck, Germany) is different (15), but is only modular during assembly. Once the system is implanted, modification or exchange is not possible. The reason for the success of the conical coupling is the fact that this mechanism contains a self-clamping effect that keeps the components always very well connected to each other. The tightness of the coupling will increase more when the patient starts to load the prosthesis. Another advantage of the conical coupling is that the components are always well centered. An additional bolt or lip is used to prevent rotation.

0391-3988/304-07 $03.50/0

However, the conical coupling has some disadvantages. Due to the conical shape, high stresses are created which could lead to crack formation (10). Also, it is difficult to detach the coupling when parts have to be exchanged. A third disadvantage is that connecting and disconnecting requires extension of the prosthesis by 25 - 60 mm. This extension may lead to damage of the surrounding soft tissue (muscles, nerves, blood vessels). A last disadvantage is that the coupling is long. This makes it impossible to use short modules.

The general risk of modular prostheses is that each coupling is a new site for fretting, disassociation, corrosion, and wear (10, 16, 17).

To overcome the disadvantages of the existing couplings, four new couplings were developed, all based upon a design of Verkerke et al (7), see Figure 1. The spacial feature of this type of coupling is that it is coupled by a lateral movement. After connecting the two parts with a bolt, it most likely will not show any relative movement of the two connecting parts during loading and unloading of the prosthesis, especially when the coupling is made from Ti-6Al-4V which has a high friction coefficient of 0.8, and so most likely there is no risk of wear as a consequence of movement. Because this coupling requires no elongation for assembly and disassembly, damage to the surrounding soft tissue structures (muscles, nerves, blood vessels) will be prevented. Assembling and disassembling is easier to perform, because the load does not act in the direction of translation. Due to the compact design, small modules are feasible.

Although this type of coupling seems to fulfill most requirements, strength and wear rate could not be judged. Therefore two-dimensional numerical models of all four designs were developed using the finite element method to determine strength and movements during loading.

The numerical models and the results of the simulations are presented in this paper.

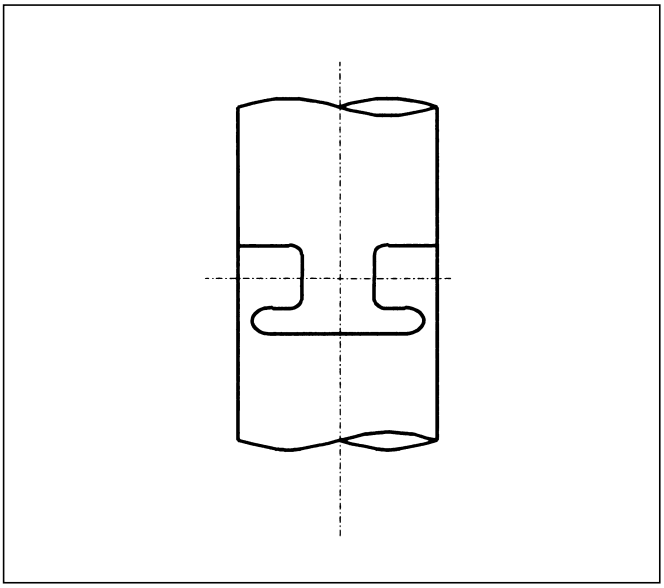

Fig. 1 - *Schematic drawing of coupling A. The horizontal dotted line represents the working line of the bolt, which pulls the two parts together.*

METHODS

To investigate the mechanical behavior of each coupling the finite element program ANSYS was used. The original coupling of Verkerke (further specified as coupling A) is represented in a two-dimensional model for modelling radial and axial loading and presented in Figure 2. For reasons of symmetry only half of the coupling was modelled. Symmetrical boundary conditions are present at the right side of parts I and II. Part II also has boundary conditions at the bottom to give the model a fixed position in the coordinate system of ANSYS. In case of an eccentric axial force, a different model is used (Fig. 2), because this loading type is not symmetrical.

Machining tolerances are taken into account by assuming a gap of 0.05 mm between parts I and II. Part I is connected to part II by a bolt which is represented by force F.

Considering the working direction of the loads, a two-dimensional model approximates the three-dimensional reality sufficiently accurately. Two-dimensional solid triangular elements with a quadratic displacement and plane strain behavior are used (PLANE 2). Point-to-surface contact elements are used (CONTAC48) to model the contact between part I and II. To simulate friction behavior, elastic coulomb friction is assumed. Finite element distribution is more dense in those areas where there are great stresses and thus large stress variations are to be expected. (Fig. 3).

The first variation of coupling A is shown in Figure 4. In this coupling B, a dovetail coupling, contact is forced to occur at the flat surfaces. Stress concentrations in the corners cannot occur because the inside radius is less than the outside radius. The wedge shape will eliminate play more effectively when the bolt is tightened.

To improve equal stress distribution a third coupling, coupling C (Fig. 5), was designed. To realise a contact area over the total radius the gap at the bottom right was enlarged to 0.1 mm and the bottom line of part II was given an angle of 1° making the gap on the left bigger than on the right. In this model the bolt force was applied at a different location than in the previous models.

To investigate if peak stresses can be decreased by applying an elastic layer on the contact surface of one of the two parts, coupling B was provided with a 0.4 mm thick inlay of PE, resulting in coupling D (Fig. 6). Characteristics of the four couplings are summarised in Table I.

All four models were loaded with axial centric and eccentric forces. Both normal loads and peak loads were considered. All models were investigated for strength and relative movement during loading. First a radial load of 1251 N was applied, caused by the bolt that connects the two parts together and eliminates play. Then a normal axial force of 3 kN was applied, a peak axial force of 10.6 kN, a normal eccentric axial force of 0.8 kN, and a peak eccentric axial force of 6.4 kN (eccentricity 50 mm), the maximum expected loads (6). All loads were applied as a single point force and were corrected for the different geometry of the two-dimensional models.

To judge strength and relative movement, material properties were implemented. Fatigue strength of Ti-6Al-4V, the preferred material, is 617 MPa, peak strength is 750 MPa, Young's modulus is 115.000 MPa, friction coefficient 0.8 (6). For the fourth coupling, PE-properties have to be considered as well: peak strength is 27 MPa, Young's modulus is 1300 MPa, friction coefficient between PE and Ti-6Al-4V is 0.3. All four models were judged according to the following criteria:

- To prevent plastic deformation that could lead to failure of the coupling, Von Mises stresses should not exceed the fatigue strength when a coupling is loaded with the normal axial or eccentric axial load;
- Von Mises stresses should not exceed the peak strength when loaded with the peak axial or eccentric axial load;
- To prevent wear, no relative movement should occur at the contact surface between the two parts of the coupling when it is subjected to normal loads. The accuracy of the locations of the nodes is ± 0.5 µm, so displacements up to 0.5 µm are considered to be 0.

A sensitivity analysis was performed for the centric load situations to determine the influence of bolt force and friction coefficient. This analysis should provide information on the functioning of the coupling when the bolt force differs from the assumed 1251 N and when friction coefficient differs from the assumed 0.8, for instance due to the presence of blood on the titanium surfaces. In all situations, first the bolt force was changed from 1251 to 1000 and 1500 N, then the friction coefficient from 0.8 to 0.4 and 0.6.

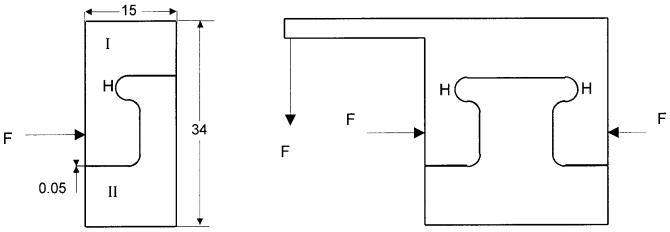

Fig. 2 - *Finite element models applied for axial loading (left) and eccentric loading (right).*

RESULTS

The locations of the maximum stresses are marked with 'H' in Figures 2, 4, 5, and 6.

In Figure 7 the maximum stresses caused by axial loads are displayed. Only coupling C shows stresses above the fatigue stress, A and B show stresses below 617 MPa. Coupling A shows the lowest stresses. Stresses in coupling D exceed those in coupling B. So instead of improving, PE-inserts worsen coupling B.

The maximum relative displacement at the contact surface when the models are loaded with a radial load of 1251 N and a normal axial load of 3 kN is 15.3, 0.4, 0.8, and 0.8 µm for coupling A, B, C, and D, respectively. Coupling A shows large displacements, while the displacement of the other couplings is very limited (C and D) or even 0 (B).

Because coupling D does not improve the results of coupling B, coupling D is no longer considered.

Figure 8 shows the maximum stresses when an eccentric axial force is applied. Again coupling A appears to have the lowest stresses. Stresses in coupling B remain below the limits; stresses in coupling C exceed the limit when normal loaded. The maximum displacement under an eccentric axial force is 8.6, 0.8 and 11.0 µm for coupling A, B and C, respectively. So coupling B shows hardly any displacement, while in coupling A and C large displacements occur.

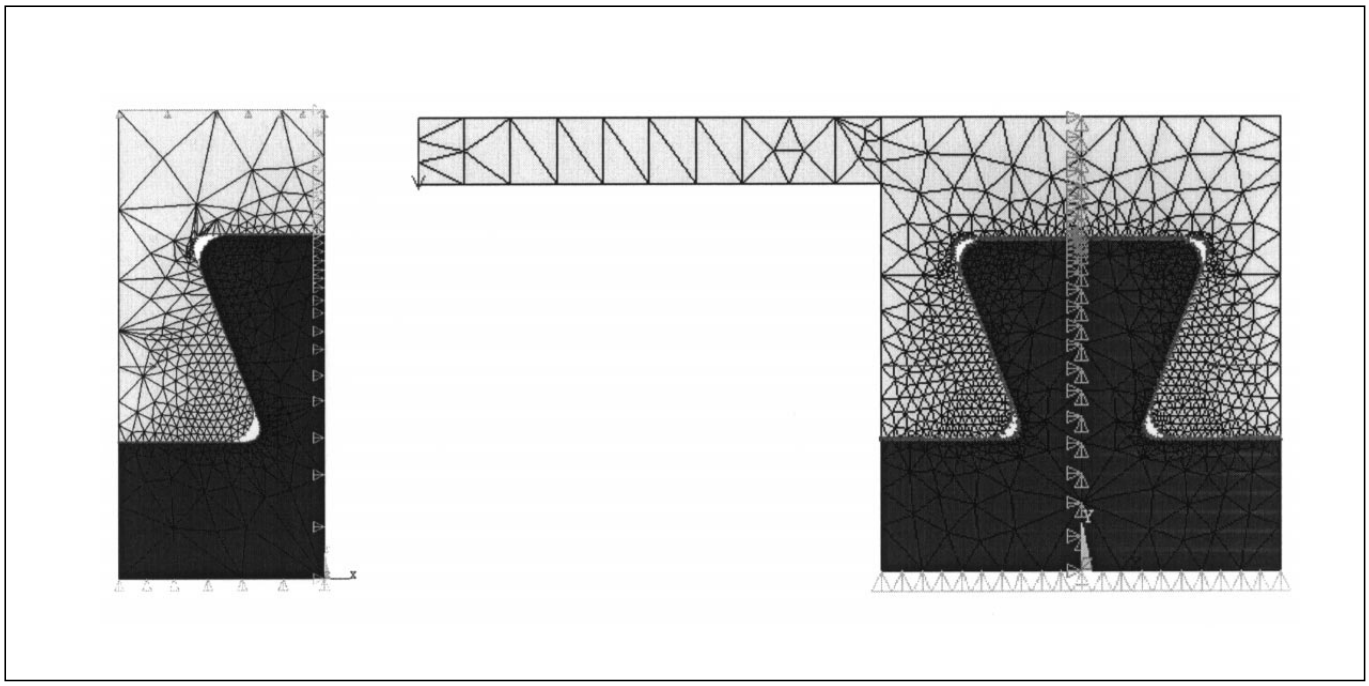

Fig. 3 - *Representation of coupling A for numerical simulation: symmetrical model (left) for analysis of radial and axial loading and a non-symmetrical model (right) for analysis of an eccentric axial force.*

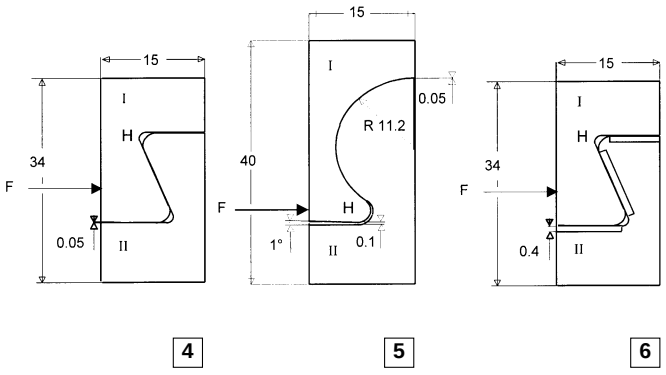

Fig. 4 - *Representation of coupling B for numerical simulation.*
Fig. 5 - *Representation of coupling C for numerical simulation.*
Fig. 6 - *Representation of coupling D for numerical simulation.*

Results from the sensitivity analysis are presented in Figures 9-12. Figures 9 - 11 show the maximum stresses in couplings A, B and C, respectively, when a radial, a radial and normal axial, and a radial and peak axial load is applied and the radial load is varied from 1000 via 1251 to 1500 N. When a radial, a radial and normal axial, and a radial and peak axial load is applied and the friction coefficient is varied from 0.4 via 0.6 to 0.8, maximum stresses do not change. The maximum displacements in coupling A under a radial and normal axial load is presented in Figure 12 for the three different radial loads and the three different friction coefficients. Displacements of coupling B and C did not change when radial load and friction coefficient was varied.

TABLE I -CHARACTERISTICS OF THE FOUR COUPLINGS

coupling	shape	length (mm)	Contacting materials	Advantage	Disadvantage
A	I	34	Ti-6Al-4V on Ti-6Al-4V	Limited peak stresses	
B	Z	34	Ti-6Al-4V on Ti-6Al-4V	Less play	
C	O	40	Ti-6Al-4V on Ti-6Al-4V	Equal stress distribution	
D	Z	34	Ti-6Al-4V on PE	Limited peak stresses, less play	PE-particle release

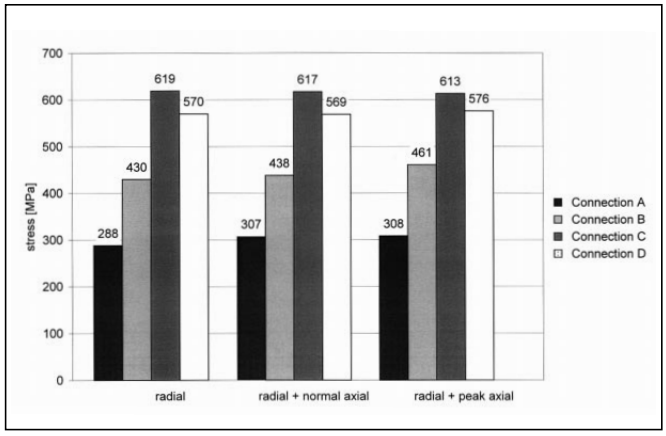

Fig. 7 - *Peak stresses (MPa) in all four couplings under three different centric loading conditions.*

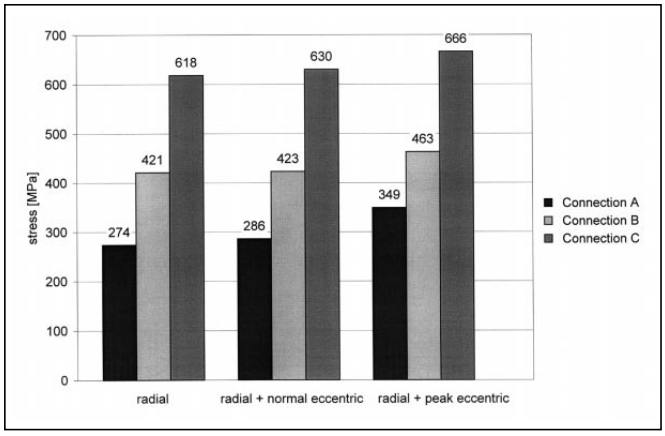

Fig. 8 - *Peak stresses (MPa) in coupling A, B and C under three different eccentric loading conditions.*

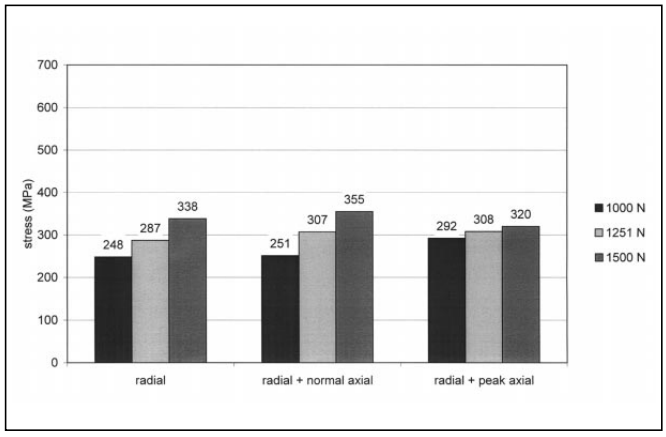

Fig. 9 - *Peak stresses (MPa) in coupling A under three different centric loading conditions and three different radial loads.*

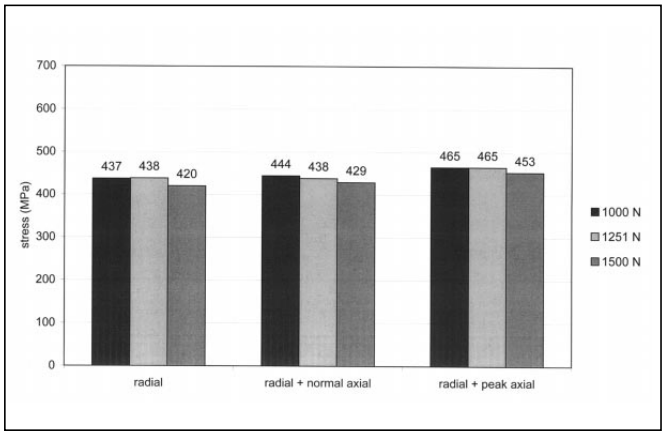

Fig. 10 - *Peak stresses (MPa) in coupling B under three different loading conditions and three different radial loads.*

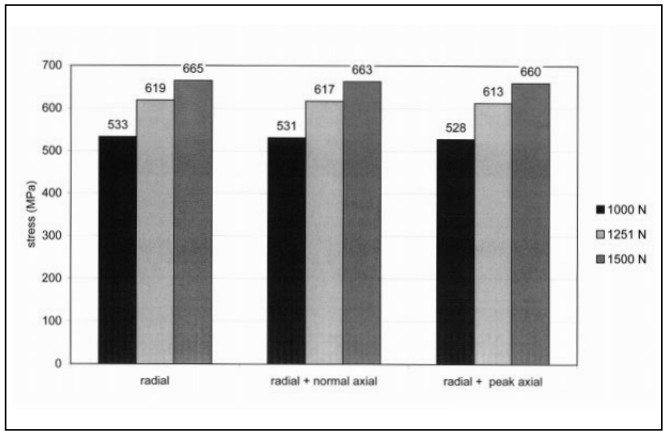

Fig. 11 - *Peak stresses (MPa) in coupling C under three different loading conditions and three different radial loads.*

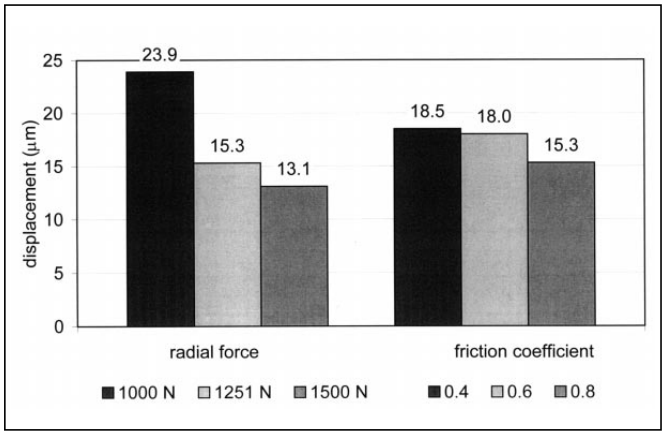

Fig. 12 - *Displacements (µm) in coupling A under three different radial loads and three different friction coefficients.*

DISCUSSION

The use of the conical coupling is widespread. Besides coupling the various modules of an endoprosthetic system for tumor management, it is frequently used for coupling the ball head of a hip joint prosthesis to the neck of the prosthesis (16).

The four designs of a coupling system presented intended to offer an improved coupling system. However, proving which of the four systems is superior to the others should require extensive and long-lasting *in-vitro* tests. Numerical modelling, is a good alternative of which the Finite Element Method is applied on a routine base for analysis of the mechanical behavior of complex structures.

When the Finite Element Method is applied on the four coupling systems presented, a clear distinction becomes apparent.

The intended improvement of coupling D versus coupling B cannot be maintained. Instead of smoothing peak stresses, increased peak stresses are found. Also, the relative displacement is larger, most probably as a result of PE-deformation. This introduces an extra disadvantage, because PE-particles cause more tissue reaction than particles of Ti-6Al-4V. Another disadvantage of this coupling is the higher production costs. The reason for this unexpected behavior of coupling D is that the PE-deformation allows more bending of the two lips of part I and thus introduces higher bending stresses in the top left corner of the coupling (marked with 'H' in Fig. 6). Coupling D was therefore rejected.

When the couplings are loaded axially, Von Mises stresses remain below the safety limits. When the couplings are loaded eccentrically, normal stresses in coupling C exceed the fatigue limit.

When considering relative displacements, coupling A and C clearly show displacements of 8.6 up to 15.3 µm, whereas coupling B show no displacement.

From the four couplings presented it is obvious, that coupling B is the best.

Coupling B meets the requirements in most conditions, with only the displacement under normal eccentric loading slightly too high. The element stresses in coupling A are the lowest of all couplings, but the displacements when the normal axial load and a normal eccentric load is applied are not equal to zero. Coupling C does show peak stresses in some elements above the fatigue stress. Also, the displacements in this coupling are not equal to zero.

When considering axial loading, stresses in couplings A and B increase when the load increases. In coupling C the opposite occurs. The reason for this phenomenon is that in couplings A and B peak stresses occur in the top left corner of the coupling (marked with 'H' in Figs. 3 and 4), whereas in coupling C peak stresses occur in the region of the radial load (marked with 'H' in Fig. 5), which is less sensitive to changes in axial loads.

When considering relative displacements, coupling A is the only one with high values and the only one without a wedge shape. This shape ensures that the bolt pulls the two parts (I and II) together in a vertical direction.

When considering eccentric loading, stresses in coupling A increase more than in the other couplings. Again, this is caused by the fact that play in a vertical direction is not eliminated by the bolt. In this load situation, coupling C shows an increase of peak stresses, which is in contrast with the previous (symmetrical) loading situation. Peak stresses now occur because the eccentric force introduces a bending moment.

When considering changes in radial (bolt) force and friction coefficient, coupling B appears to be insensitive. Relative displacements remain unchanged. Its wedge shape gives it good clamping properties. Because stresses never rise above the fatigue stress, coupling B is very stable.

Coupling C is also not sensitive to changes in radial force and friction coefficient. Relative displacements hardly change. However, coupling C does show stresses above the fatigue stress when the radial force is increased to 1500 N.

Coupling A is less stable and shows extra movement when the friction coefficient or the radial force decreases. When the radial force increases the displacements are still far from zero so changing this parameter does not improve the coupling.

Each model is an abstraction of reality. Assumptions and simplifications are necessary to be able to create a model. The assumption that a finite number of elements is sufficient for an accurate prediction of stresses, and displacements can be checked by considering the stress changes within one element. If these changes are limited, enough elements have been used. In all four models, the elements were chosen small enough to fulfill this requirement, except for some elements with stresses that could clearly be identified as extreme values. Another possibility to check the accuracy of the models is to compare stresses under radial loading as has been calculated with the symmetrical and the complete model (first series of columns in Figs. 7 and 8, respectively). Stresses in the symmetrical model are somewhat higher than in the complete model, but the

differences are limited (0.2 - 4.9%).

A major simplification is the two-dimensional nature of the model. However, considering the working direction of the loads, the model will approximate the three-dimensional reality accurately enough. Although the modelling of external forces and bolt forces as single point force is a simplification, at the critical parts of the coupling, the contact region between parts I and II, the single point force already is distributed over a large number of elements, thus resembling reality to a large extent.

In spite of the necessary simplifications and assumptions, the numerical model according to the Finite Element Method has proved to be an accurate tool in predicting the mechanical behavior of the four couplings considered.

CONCLUSIONS

Coupling B is a good alternative to a conical coupling. Relative displacements are zero, stresses remain within the safety limits. The lateral assembling enables short modules and prevents soft tissue damage.

Reprint resquests to:
Bart Verkerke, MSc PhD
University of Groningen
Department of Biomedical Engineering
P.O. Box 196
9700 AD Groningen
The Netherlands
e-mail: g.j.verkerke@med.rug.nl

REFERENCES

1. Schraffordt Koops H, Oldhoff J, Veth RPH, et al. New developments in the treatment of osteosarcoma of the extremities. Oncology (Life Sci Adv) 1990; 915-8.
2. Veth RPH, Nielsen HKL, Oldhoff J, et al. The treatment of primary tumors of the femur with chemotherapy (if indicated), resection and reconstruction with an endoprosthesis. J Surg Oncol 1985; 30: 252-8.
3. Kenan S, Bloom N, Lewis MM. Limb-sparing surgery in skeletally immature patients with osteosarcoma; the use of an expandable prosthesis. Clinical Orthopaedics and Related Research 1991; 270: 223-30.
4. May DRW, Walker PS. Design and follow-up of extending prosthetic replacements for children. In: Brown KBL, ed. Complications of limb salvage: prevention, management and outcome. Montreal: ISOLS, 1991; 505-10.
5. Schiller C, Windhager R, Fellinger EJ, Salzer-Kuntschik M, Kaider A, Kotz R. Extendable tumor endoprostheses for the leg in children. Journal of Bone and Joint Surgery - Series B 1995; 77(4): 608-14.
6. Verkerke GJ, Schraffordt Koops H, Veth RPH, et al. Design of a lengthening element for a modular femur endoprosthetic system. Proceedings Institution of Mechanical Engineers, Part H. Journal of Engineering in Medicine 1989; 203: 97-102.
7. Verkerke GJ, Schraffordt Koops H, Veth RPH, et al. An extendable modular endoprosthetic system for bone tumor management in the leg. Journal of Biomedical Engineering 1990; 12: 91-6.
8. Verkerke GJ, Schraffordt Koops H, Veth RPH, Horn JR van, Postma L, Grootenboer HJ. First clinical experience with a noninvasively extendable endoprosthesis: A limb-saving procedure in children suffering from a malignant bone tumor. Int J Artif Organs 1997; 21(5): 413-7.
9. Capanna R, Guerra A, Ruggieri P, Biagini R, Campanacci M. The Kotz modular prosthesis in massive osteo-articular resections for bone tumor. Italian Journal of Orthopaedics and Traumatology 1985; 11(3): 271-81.
10. Collier JP, Mayor MB, Jensen RE, et al. Mechanisms of failure of modular prosthesis. Clinical Orthopaedics and Related Research 1992; 285:129-39.
11. Kotz R, Ritschl P, Trachtenbrodt J. A modular femur-tibia reconstruction system. Orthopedics 1986; 9(12): 1639-52.
12. Zwart HJJ, Tamilan AHM, Schimmel JW, Horn JR van. KOTZ modular femur tibia reconstruction (KMFTR). Acta Orthopedica Scandinavica 1994; 3: 315-8.
13. Ward WG, Dorey F, Eckardt JJ. Total femoral endoprosthetic reconstruction. Clinical Orthopaedics and Related Research 1995; 316: 195-206.
14. Ward WG, Yang RS, Eckardt JJ. Endoprosthetic bone reconstruction following malignant tumor resection in skeletally immature patients. Orthopedic Clinics of North America 1996; 27(3): 493-502.
15. Nieder E, Engelbrecht E, Steinbrink K, Keller A. Modulares System für den Femurtotalersatz - Endo-Modell®. Der Chirurg: Zeitschrift für alle Gebiete der operativen Medizin. 1983; 54(6): 391-9.
16. Collier JP, Mayor MB, Williams IR, Surprenant VA, Surprenant HP, Currier BH. The tradeoffs associated with modular hip prosthesis. Clinical Orthopaedics and Related Research 1995; 311: 91-101.
17. Viceconti M, Baleani M, Squarzoni S, Toni A. Fretting wear in a modular neck hip prosthesis. Journal of Biomedical Materials Research 1997; 35: 207-16.